

# International Journal of Pharmaceutics

## Hydroxytyrosol oleate: a promising neuroprotective nanocarrier delivery system of oleuropein and derivatives

--Manuscript Draft--

|                              |   |
|------------------------------|---|
| <b>Manuscript Number:</b>    | IJPHARM-D-22-02910R1  |
| <b>Article Type:</b>         | Review Article  |
| <b>Keywords:</b>             | Hydroxytyrosyl oleate; Olive Phenols; Oleuropein; 3,4-DHPEA-EA; Hydroxytyrosol; Nanoparticles   |
| <b>Corresponding Author:</b> | Monica Nardi<br>Magna Graecia University of Catanzaro<br>Germaneto, Catanzaro ITALY   |
| <b>First Author:</b>         | Monica Nardi  |
| <b>Order of Authors:</b>     | Monica Nardi<br>Steve Brocchini<br>Satyanarayana Somavarapu<br>Antonio Procopio   |
| <b>Abstract:</b>             | <p>Olive Phenols (OPs) are known to be potent antioxidants and possess various bioactivities and health benefits. Epidemiological studies suggest that consumption of olive oil reduces the risk of different diseases exerting a protective effect against certain malignant tumors (prostate, breast, digestive tract, endothelium, etc...) but the extremely low absorption rate of olive phenolic compounds restricts their bioactivity. In this context, solid lipid nanoparticles (SLNs) are a promising solution because they provide higher drug stability and can incorporate both lipophilic and hydrophilic drugs. Interesting experimental results have been obtained using hydroxytyrosol oleate (HtyOle) as a delivery system for the synthesis of nanoparticles containing oleuropein (OL), oleuropein aglycone (3,4-DHPEA-EA), and hydroxytyrosol itself (Hty). In this work, hydroxytyrosol oleate (HtyOle) and hydroxytyrosol oleate (HtyOle)-based solid lipid nanoparticles were prepared and characterized. In addition, we evaluated in vitro their antioxidant activity by DPPH assays and by ROS formation using the SH-SY5Y cell line.</p> |
| <b>Suggested Reviewers:</b>  | Donato Cosco<br>donatocosco@unicz.it<br><br>Carlos Alberto Afonso<br>carlosafonso@ff.ulisboa.pt<br><br>Fresta Massimo<br>fresta@unicz.it<br><br>Fabio Mazzotti<br>fmazzotti@unical.it<br><br>Leonardo Di Donna<br>l.didonna@unical.it   |

1 **Hydroxytyrosol oleate: a promising neuroprotective nanocarrier delivery system of oleuropein**  
2 **and derivatives**

3 Monica Nardi,<sup>a,b\*</sup> Steve Brocchini,<sup>a</sup> Satyanarayana Somavarapu<sup>a</sup> Antonio Procopio<sup>b</sup>

4

5 *<sup>a</sup> Department of Pharmaceutics, UCL School of Pharmacy, 29–39 Brunswick Square, London*

6 *WC1N 1AX, UK*

7 *<sup>b</sup> Department of Health Sciences, Università “Magna Græcia” di Catanzaro, Viale Europa – Campus*

8 *Universitario “S. Venuta” – Loc. Germaneto - 88100 (CZ), ITALY.*

9

10

11

12 **\*Corresponding Author:**

13 Professor Monica Nardi

14 Università “Magna Græcia” di Catanzaro

15 Dipartimento di Scienze della Salute

16 Viale Europa, Germaneto - 88100 Catanzaro – Italy

17 Tel. +39 0961 3694116; Fax. +39 0961 3694237; e-mail: monica.nardi@unicz.it

18

19

20

21

22

23

24

25

26 **Abstract**

27 Olive Phenols (OPs) are known to be potent antioxidants and possess various bioactivities and health  
28 benefits. Epidemiological studies suggested that consumption of olive oil reduces the risk of different  
29 diseases exerting a protective effect against certain malignant tumors (prostate, breast, digestive tract,  
30 endothelium, etc.). However, extremely low absorption rate of olive phenolic compounds restricts  
31 their bioactivity. In this context, solid lipid nanoparticles (SLNs) are a promising solution because  
32 they provide higher drug stability and can incorporate both lipophilic and hydrophilic drugs.  
33 Interesting experimental results have been obtained using hydroxytyrosol oleate (HtyOle) as a main  
34 component of a nanoparticle delivery system containing oleuropein (OL), oleuropein aglycone (3,4-  
35 DHPEA-EA), or hydroxytyrosol itself (Hty). In this work, hydroxytyrosol oleate (HtyOle) and  
36 hydroxytyrosol oleate (HtyOle)-based solid lipid nanoparticles were prepared and characterized. In  
37 addition, we evaluated *in vitro* their antioxidant activity by DPPH assays and by ROS formation using  
38 the SH-SY5Y cell line.

39 **Keywords**

40 Hydroxytyrosyl oleate, Olive Phenols, Oleuropein, 3,4-DHPEA-EA, Hydroxytyrosol, nanoparticles

41

42

43

44

45

46

47

## 48 **1. Introduction**

49 The food industries produce large amounts of waste, which represent disposal and potentially  
50 environmental pollution problem. Efficient, inexpensive, and environmentally friendly utilization of  
51 wastes is becoming more important. New methods for the handling and treatment of these materials  
52 have been introduced in the recovery, bioconversion, and utilization of valuable constituents from  
53 these wastes (Okonko et al. 2009).

54 Olive oil is an important component of the Mediterranean diet, containing variable amounts of  
55 triacylglycerols and small quantities of free fatty acids, glycerol, pigments, aroma compounds, sterols,  
56 tocopherols, phenols, unidentified resinous components and others. It is recognized that the well-  
57 known pharmacological properties of micro-components of olive oil, olive fruit, and leaves are  
58 ascribable to their phenolic content. During the olive oil production process, the major proportion of  
59 the phenolic compounds [oleuropein (OL) and its metabolites as 3,4-dihydroxyphenylethanol-  
60 elenolic acid dialdehyde (3,4-DHPEA-EDA), 3,4-dihydroxyphenylethanol-elenolic acid (3,4-  
61 DHPEA-EA) and hydroxytyrosol] are found in the waste. Several *in vitro* and *in vivo* studies confirm  
62 that phenolic compounds exert multiple biological activities, such as antioxidant (Visioli et al. 1998,  
63 Nardi et al. 2014, Rizzo et al. 2017), antiatherogenic (Karantonis et al. 2006), angiotensin-converting  
64 enzyme (ACE) inhibitory (Kiss et al., 2008; Alcaide- Hidalgo et al. 2020), antimicrobial (Guo et al.  
65 2019) anti-inflammatory (Sindona et al. 2012), and anticancer (Giada et al. 2019, Campolo et al.  
66 2012). However, the hydrophilicity of olive phenolic compounds restricts to a great extent their  
67 application in lipophilic systems.

68 In the last decade, Procopio et al. (Procopio et al., 2011) reported that several derivatives of oleuropein,  
69 the predominant phenolic component in the olive leaves, such as oleuropein aglycone, hydroxytyrosol,  
70 and their acetylated lipophilic forms, can be prepared by simple and environmentally friendly  
71 semisynthetic protocols. Thus, lipophilic oleuropein aglycone derivatives were synthesized and  
72 evaluated in terms of their lipophilicity and antioxidant capacity. The biological activities of these

73 derivatives were directly related to their level of lipophilicity, with the maximum antioxidant and  
74 neuroprotective activity reported for the oleyl derivative (Nardi et al. 2017).

75 Another excellent strategy to increase the bioavailability of biologically active compounds could be  
76 encapsulation in nanoparticles (NPs) (Yang et al. 2020). These spherical particles are an alternative  
77 drug delivery system to classical carriers and an excellent candidate for the encapsulation of drugs  
78 with poor bioavailability. The solid lipid nanoparticles (SLNs) are typically spherical with an average  
79 diameter between 10 and 1000 nanometers and contain a hydrophobic solid matrix core with one  
80 layer of a lipid coating (Ekambaram et al. 2012; Pardeike et al. 2009).

81 In this way, drugs are co-processed with a surfactant to be formulated into stabilized nanosuspensions  
82 and are made suitable for pharmacological treatments (Scioli Montoto et al. 2020). Clinical use of  
83 SLNs, however, required toxicological risk assessment, and the toxicological and inflammatory  
84 potential of SLNs was investigated using *in vitro*, *ex vivo*, and *in vivo* methods (Nassimi et al. 2010)  
85 that have indicated the cancer treatment as the most relevant field of application (Hare et al. 2017).

86 However, the low efficacy and lack of selectivity can cause severe side effects for health issues.  
87 Furthermore low drug loading capacity, the carrier's toxicity (the carrier is usually the major  
88 component of the formulation) and its biodegradation can be a potential problem for pharmaceutical  
89 therapy (Tapeinos et al. 2017).

90 Considering our wide experience and our research studies on the phenolic compounds of olive  
91 (Procopio et al. 2009; Impellizzeri et al. 2011; Nardi et al. 2020; Mazzei et al. 2020; Mancuso et al.  
92 2021), we synthesized a new carrier-free drug system using hydroxytyrosol oleate as solid lipid in the  
93 synthesis of nanoparticles containing phenolic compounds (PCs) as OL, 3,4-DHPEA-EA and Hty  
94 (Figure 1).

95 Please Insert the Figure 1 here

96 The hydroxytyrosyl esters are known for their ability to reduce nitric oxide (NO) production,  
97 especially in the case of the oleyl derivative HtyOle. This conjugate was an excellent topical  
98 therapeutic agent to treat skin diseases due to his permeation profile through the human stratum  
99 corneum and viable epidermis membranes (Procopio et al. 2011).

100 The HtyOle was identified in olive oil by-products by high performance liquid chromatography  
101 coupled with mass spectrometry (Plastina et al. 2019) and its antioxidant capacity was tested in  
102 human keratinocytes (Benincasa et al. 2020). The compound was synthesized by the modified  
103 Lewis catalysis method proposed by Procopio et al. (Procopio et al. 2011) using 2-Me THF as green  
104 solvent. The 2-Me THF can be produced from natural sources (corncoobs or bagasse) and recently  
105 tested as an excellent reaction medium for the synthesis of organic molecules involving the use of  
106 Lewis acid catalysis (Nardi et al. 2015; Nardi et al. 2017).

107 The nanoparticles obtained (SLN-HtyOle, SLN-HtyOle-OL, SLN-HtyOle-3,4-DHPEA-EA and  
108 SLN-HtyOle-Hty respectively), were tested on neuroblastoma SH-SY5Y cell line evaluating the  
109 antioxidant proprieties by ROS formation and using the DPPH (1,1-diphenyl-2-picrylhydrazyl)  
110 assay (Xie et al. 2014).

111 Aim of the work was to show the greater bioavailability of encapsulated phenolic compounds using  
112 hydroxytyrosyl oleate-based solid lipid nanoparticles and the greater capacity for scavenging  
113 radicals in the biological environment.

114

## 115 **2. Materials and methods**

### 116 *2.1. Materials*

117 Hydroxytyrosol was purchased from TCI AMERICA (Purity: >98.0% (GC)). The DPPH was  
118 purchased from Eastman Organic Chemical (Rochester, NY) and all other chemicals were purchased  
119 from Sigma (Sigma-Aldrich, Milan, Italy), unless otherwise specified.

## 120 2.2. Synthesis of *HtyOle*

121 The hydroxytyrosol oleate was prepared using a slightly modified synthesis protocol reported by  
122 Procopio et al. (Procopio et al. 2011). To a solution of hydroxytyrosol (1.62 mmol) in 2-MeTHF (8  
123 mL) 1 equiv of oleyl acid chloride (1.62 mmol) and Er(OTf)<sub>3</sub> (0.0162 mmol) were added under  
124 stirring (Heidolph 505-20000-00 Hei-Standard, Kintail House, Inverness-shire, IV2 3BW, United  
125 Kingdom). The mixture reacted for 12 h at room temperature (25 °C). After completion, the reaction  
126 mixture was extracted with H<sub>2</sub>O and then, the organic phase was dried over Na<sub>2</sub>SO<sub>4</sub>. The crude  
127 material, dried under vacuum (Hei-VAP Advantage Rotary Evaporator, Heidolph, Germany) (~1  
128 mmHg), was purified by flash chromatography (mobile phase CHCl<sub>3</sub>/MeOH, 9.5/0.5, 90% yield) and  
129 identified by TLC and NMR analyses (Bruker Avance 500 MHz NMR spectrometer equipped with a  
130 QNP (<sup>31</sup>P, <sup>13</sup>C, <sup>15</sup>N and <sup>1</sup>H) cryoprobe). <sup>1</sup>H-NMR and <sup>13</sup>C-NMR showed the *HtyOLE*

131 Hydroxytyrosol oleate (*HtyOLE*): <sup>1</sup>H-NMR (500 MHz, CDCl<sub>3</sub>) δ= 0.88 (3H, CH<sub>3</sub>, t, J = 5.0 Hz), 1.30  
132 (14H, 7CH<sub>2</sub>, m), 1.60 (2H, CH<sub>2</sub>, m), 1.98 (4H, CH<sub>2</sub>-C=C-CH<sub>2</sub>, dd, J=5, J=10), 2.28 (1H, CHCO, t, J  
133 = 7.6 Hz), 2.35 (1H, CHCO, t, J = 7.6 Hz), 2.82 (2H, CH<sub>2</sub>Ph, t, J = 7.2 Hz), 4.23 (2H, CH<sub>2</sub>OCO, t, J  
134 = 7.3 Hz), 5.35 (2H, CH=, m), 6.65 (1H, CH<sub>ar</sub>, dd, J = 3.1, 1.9 Hz), 6.76 (2H, CH<sub>ar</sub>, dd, J = 8.0, 1.9  
135 Hz); <sup>13</sup>C-NMR (500 MHz, CDCl<sub>3</sub>) δ= 14.1, 22.7, 25.0, 27.7, 29.3, 29.4, 29.7, 29.9, 31.9, 33.9, 34.8,  
136 115.9, 116.4, 122.8, 130.6, 144.5, 145.6.

## 137 2.3. *Oleuropein* Extraction

138 The MW-assisted extraction of oleuropein (Procopio et al. 2009) was performed on several samples  
139 of olive leaves from Coratina cultivar of *Olea europaea* L, dried for 48 h at 50 °C, milled, and kept  
140 at r.t. until use (Costanzo et al. 2017).

141 *2.4. Synthesis of 3,4-DHPEA-EA.*

142 Oleuropein (740 mg, 1.34 mmol) was dissolved in aqueous CH<sub>3</sub>CN (12.7 mL) in the presence of  
143 Er(OTf)<sub>3</sub> (123.5 mg, 0.20 mmol) and refluxed at 80 °C for 8 h. At the end of the conversion, the  
144 hydrolysate was cooled, 5 mL of water was added, and the mixture was extracted with CH<sub>2</sub>Cl<sub>2</sub>. After  
145 drying on Na<sub>2</sub>SO<sub>4</sub>, the organic solvent was removed in vacuo and the crude product was purified by  
146 flash chromatography (mobile phase CH<sub>2</sub>Cl<sub>2</sub>/MeOH 8:2 v/v) and identified by TLC, and NMR  
147 analyses (Procopio et al. 2009).

148 *2.5. Preparation of Oleuropeine (SLN-HtyOle-OL), Hydroxytyrosol (SLN-HtyOle-Hty), 3,4-*  
149 *DHPEA-EDA (SLN-HtyOle-3,4-DHPEA-EA) loaded Hydroxytyrosol oleato nanocarriers.*

150 Nanoformulations were prepared employing a modified thin-film hydration method (Zupančić et al.  
151 2014). OL, Hty and 3,4-DHPEA-EDA (5 mg) within the presence of HtyOle (37.5 mg) and Lutrol<sup>®</sup>  
152 micro 68 (37.5 mg) were individually dissolved in 10 mL of CH<sub>2</sub>Cl<sub>2</sub> using flask (50 mL). Each  
153 mixture was sonicated for a 1 min employing a VWR ultrasonic cleaner bath USC300T (VWR  
154 International Limited, UK). The mixture was evaporated under vacuum employing a rotary  
155 evaporator (Hei-VAP Advantage Rotary Evaporator, Heidolph, Germany) until a skinny film was  
156 obtained. The resultant thin film, present within the flask, was immediately dispersed in 10 mL of  
157 H<sub>2</sub>O at temperature (25 °C) for 1-2 minutes, then sonicated for an extra 1 min until the film was fully  
158 removed and dispersed within the water.

159 After the purification by means of Amicon<sup>®</sup> Ultracentrifugal Filters (cut-off 10 KDa, 4000 rpm for  
160 60 min), the SLN-HtyOle-OL, SLN-HtyOle-HTy and SLN-HtyOle-3,4-DHPEA-EA dispersions  
161 were dried by freeze-drying process employing a Virtis AdVantage 2.0 BenchTop freeze-dryer (SP  
162 Industries, UK) for further analysis. A measurement of PCs recovery during filtration has been made  
163 (See supporting information). SLN-HtyOle nanoformulations were prepared as described above and  
164 used as an impact treatment within the cellular assays.



165 *2.6. Particle size distribution and zeta potential measurements*

166 The particule size and zeta potential of SLN were measured using Malvern Zetasizer NanoZS  
167 (Malvern Instruments, UK). Three independent measurements were performed on each sample. The  
168 samples were diluted appropriately with the aqueous phase of the formulation at 25° C.for the  
169 measurements. Size distribution was measured via photon correlation spectroscopy (PCS) as Z-Ave  
170 hydrodynamic diameter and polydispersity index (PDI). Each formulation was prepared at least six  
171 times and measurements were taken in triplicate for each sample (Petkar et al. 2018).

172 *2.7. Percentage drug content into solid nanoparticles.*

173 The loading efficiency of the formulations was determined spectroscopically and, subsequently,  
174 confirmed using HPLC (wavelength: 255 nm; solvent: acetonitrile/water (70/30, v/v). The  
175 encapsulation efficiency (EE) and the loading capacity (LC) of the formulations were  
176 calculadetermined using the following equations.

177

$$178 \quad EE (\%) = (\text{weight of loaded compound} / \text{weight of compound in feed}) \times 100 \quad (1)$$

179 where

180 (weight of loaded compound) is the weight of encapsulated PC detected spectroscopically within  
181 the nanocarriers after 0.22 µm filtration to remove unencapsulated material

182 (weight of compound in feed) is the weight of PC originally added to the formulation.

183

$$184 \quad LC (\%) = (\text{weight of loaded compound} / \text{weight of SLNs}) \times 100 \quad (2)$$

185 where

186 weight of SLNs is total weight of HtyOle, surfactant and PC

187 SLN-HtyOle-OL, SLN-HtyOle-Hty and SLN-HtyOle-3,4-DHPEA-EA formulations (8 mg of  
188 nanoparticles) were diluted to 5 mL with methanol (0.1 mg of PC in 1ml) and were analyzed by

189 reverse-phase HPLC on a Jasco LC-NetII/ADC, UV-2075 detector to estimate OL, Hty or 3,4-  
190 DHPEA-EA content. A Luna Altech 4.6 × 150 mm Adsobosphere C18 column with 5 μm particles  
191 of bonded silica gel with a guard column (4.6 × 7.4 mm Adsobosphere C18) was used. Absorbance  
192 chromatograms were obtained at 255 nm and every one the measurements were performed at room  
193 temperature. A binary mixture of acetonitrile/water (70/30, v/v) was applied as mobile phase with a  
194 rate of flow 1 mL/min and 20 μl injection loop. The retention time was 1.2 min for OL, 1.4 min for  
195 Hty and 4.3 for 3,4-DHPEA-EA. The strategy was validated for linearity, precision and recovery  
196 employing a standard solution (200μg/mL; 140μg/mL; 100μg/mL; 70μg/mL;) of OL, Hty and 3,4-  
197 DHPEA-EA. All calibration curves (See Supporting Information) showed good linear regression ( $R^2$   
198 = 0.974;  $R^2$  = 0.962;  $R^2$  = 0.972 respectively) over the wide test ranges. The calibration curve was  
199 linear within the used solvent. the typical recovery was 99.4% for OL, 98,8% for 3,4-DHPEA-EA  
200 and 99.2% for Hty with relative variance (RSD) 0.326 %, 0,187% and 0.521 % (n = 3) (See  
201 Supporting Information, Figure S3, S4, S5).

202 The PCs release was quantified *in vitro* by a membrane dialysis tube method. 75 mg of freeze-dried  
203 samples was dissolved in 1 mL of 0.1 M Phosphate buffered saline (PBS, pH 7.4) and was placed  
204 into a cellulose acetate dialysis tube (12 kDa, diameter 6,5 mm, 0,32 mL/cm, area surface=3,30 cm<sup>2</sup>)  
205 (Spectra/Pro, Spectrum Lab, Breda, Netherlands). The dialysis bag was immersed in a flask  
206 containing 100 mL of buffer solution and stirred (1000 rpm) a 37 °C. Samples (1 mL of the dissolution  
207 medium) were taken at determined time point (1, 2, 4, 6, 8, 10, 16, 24, 36 and 48 h), diluted by adding  
208 4 mL of buffer solution and quantified by HPLC method above described. 1 mL of fresh PBS was  
209 adding to flask to the receptacle. This experiment was performed three times.

## 210 2.8. DPPH radical scavenging activity.

211 DPPH reagent standard solution: 0.0039 g of DPPH was dissolved in 100 mL of methanol to generate  
212 a 0.1 mM DPPH stock solution; working solutions were prepared fresh daily by diluting the stock  
213 solution with solvent sufficiently to reduce the absorbance at 517 nm to 1.00 (±0.02). Stock solutions

214 (100 mM) of test antioxidants were prepared in methanol, then serially diluted for progressively  
215 lowering the concentrations for testing. The stock solution of molecules encapsulated, were prepared  
216 dissolving 10 mg of SLN in 2.5 mL of water. 1 mL solution of DPPH (0.1 mM) was added to 1 mL  
217 of 100, 50, 25, 12.5, 6.25, 3.125, 1.562 and 0.78 mM of PC-loaded SLNs or free PCs (the  
218 concentration was calculated based on the respective encapsulated phenolic compound). An equal  
219 amount of methanol and DPPH served as control. After 40 min of incubation in the dark, absorbance  
220 was recorded at 517 nm and the experiment was performed in triplicate, using a Jenway 7310/7315  
221 UV Vis Scanning Spectrophotometers. The percentage scavenging was calculated using the formula:

$$222 \quad \text{Inhibition (\%)} = [(\text{Control} - \text{Test}) / \text{Control}] \times 100 \quad (3)$$

223 where control is the absorbance of the negative control (DPPH solution) and test is the absorbance  
224 of the compounds at different concentrations. The sample concentration providing 50% inhibition  
225 (IC<sub>50</sub>) was calculated by plotting the inhibition percentage vs. the sample concentration.

## 226 *2.9 Biological Tests*

### 227 *2.9.1 Cell Culture.*

228 The human SH-SY5Y neuroblastoma cell line was purchased from ATCC, The Global Bioresource  
229 Center, and maintained in Dulbecco's modified Eagle's medium (DMEM) supplemented with 5  
230 mg/mL penicillin/streptomycin, 10 mM L-Glutamine, and 10% (v/v) fetal bovine serum (FBS). Cells  
231 were kept in an incubator at 37 °C with a 5% CO<sub>2</sub> atmosphere. After two passages, the SH-SY5Y  
232 cells were plated at a density of 2x10<sup>4</sup> cells/well in a 96-well microplate for the sulforhodamine B  
233 assay (SRB) and reactive oxygen species (ROS) assays

### 234 *2.9.2 Sulforhodamine B (SRB) Cell Proliferation Assay.*

235 The *in vitro* cytotoxicity of the plain and PC-loaded SLNs (OL, HTy and 3,4-DHPEA-EA) against  
236 SH-SY5Y cells were evaluated using a SRB assay (Vichai et al. 2006). The neuroblastoma cells,

237 inoculated in 96-well microtiter plates (200  $\mu$ L at  $2 \times 10^4$  cells/well) were allowed to attach overnight.  
238 A stock solution of the nanoparticles (0.1 M in dimethylsulfoxide (DMSO)) was diluted to 0,5  $\mu$ M,  
239 1  $\mu$ M, 10  $\mu$ M and 100  $\mu$ M with the culture medium. The cell media was removed and the PC solutions  
240 added to well to achieve a final volume of 200  $\mu$ L. The obtained plates were incubated under standard  
241 conditions for 24 h. The supernatant was discarded and the cells were fixed *in situ* gently via the  
242 addition of 100  $\mu$ L of cold trichloroacetic acid (TCA) 10% (w/v) and incubated for 60 min at 4  $^{\circ}$ C.  
243 The plates were washed 5 times with double distilled water (DDW) and then air-dried. A  
244 Sulforhodamine B (SRB) solution (50  $\mu$ L) at 0.4% (w/v) in 1% acetic acid was added to each well  
245 and the plates were incubated at room temperature for 30 min. When the color appears, the excess  
246 dye was collected and the plates were washed four times with 1% acetic acid and air-dried. The  
247 bound dyes were then solubilized in a 10 mM Tris base (200  $\mu$ L of 10 mM unbuffered solution, pH  
248 10.5, Sigma) and the plate was shaken for 15 min. The absorbance was measured at 492 nm using a  
249 Spectra-Max-190 (Molecular Devices, Sunnydale, USA) microplate reader (Skehan et al. 1990). The  
250 plate-by-plate analysis of the test wells relative to control wells was used to determine percent growth,  
251 and the ratio of the absorbance in the test well to the absorbance in the control wells  $\times$  100 was  
252 calculated.

### 253 *2.9.3 ROS Formation*

254 The cells were plated at  $2 \times 10^4$  cells/well dilution in 250  $\mu$ L, in a black, flat-bottom 96-well plate  
255 (Thermo Fisher Scientific) and incubated overnight. The DMSO PC solution was added at the  
256 appropriate concentrations diluted in 100  $\mu$ L fresh culture medium and incubated for 2.5 h. 50  $\mu$ L of  
257 stock solution of 2,7-dichlorofluorescein diacetate in EtOH (DCFH-DA (5000  $\mu$ M)) was added to the  
258 wells to obtain a final concentration of 5  $\mu$ M. The plates were wrapped in aluminum foil and  
259 incubated at 37  $^{\circ}$ C. After 30 min, 100  $\mu$ L of 6-hydroxy dopamine (6-OHDP, 10000  $\mu$ M stock solution  
260 in fresh medium) was added to achieve a final concentration of 25  $\mu$ M (Zihua et al 2012) and the

261 plates wrapped in aluminum foil, incubated for an additional 24 h period, after which DCF  
262 fluorescence was read at 530 nm.

263 ROS formation data were calculated with the following equation :

264

$$265 \text{ ROS formation (\%)} = [(M.F.U. \text{ drug DMSO} + 6\text{-OHDP cells}) - (M.F.U. \text{ drug DMSO blank}) - (M.F.U. \\ 266 \text{ DMSO cells}) (M.F.U. 6\text{-OHDP cells}) - M.F.U. \text{ DMSO cells}] \times 100 \quad (4)$$

267 where

268 M.F.U. is the Mean Fluorescence Units

#### 269 2.9.4 Statistical analysis

270 The experiments were repeated thrice and the results are expressed as mean  $\pm$  standard error of the  
271 mean (SEM). The data were evaluated by one-way analysis of variance (ANOVA) followed by  
272 Tukey's test. The *in vitro* procedures were carried out with  $n = 3$ , while cell culture experiments were  
273 performed with  $n = 6$  (6 wells per group). The differences among the data were evaluated by the  
274 analysis of variance (ANOVA) followed by Tukey-test according to the statistical program  
275 SigmaStat1 (Jandel Scientific, Chicago, IL, USA). A  $p$ -value less than 0.001 was regarded as  
276 significant.

### 277 3. Results and discussion

278 The Mediterranean diet, that includes olive oil as one of the major fatty food components, has been  
279 reported to prevent and improve neurological diseases. Oleuropein is the major phenolic component  
280 present in different parts of the Olive (*Olea europaea* L.) tree. The protective role of oleuropein in  
281 preventing neurodegenerative diseases has been reported in several studies (Hornedo-Ortega et al.  
282 2018) and has been related to several mechanisms such as the enhancing of the antioxidant pool of  
283 the cerebral region and the decreasing of the release of proinflammatory cytokines and chemokines  
284 that prevents the occurrence of neuroinflammation. Oleuropein is a natural phenolic compound

285 obtained from olive leaves (waste material from the olive production chain), potentially valuable for  
286 employment as an extraordinary starting material for the generation of other natural OPs (oleuropein  
287 aglycone, oleacein and hydroxytyrosol) considered potential phenolic compounds of interesting  
288 therapeutic utility (Cavaca et al. 2017). One of the main restrictions to the therapeutic use of OPs in  
289 free radical related disorders, including neurodegenerative diseases, is their poor bioavailability  
290 (D'Archivio et al. 2010). In the current work HytOle, of more lipophilic nature than the parent  
291 compound Hty, was synthesized using an environmental-friendly and fast procedure and used as solid  
292 lipid in the formulation of SLN-HytOle, containing OL, 3,4-DHPEA-EA or Hty. The obtained  
293 nanoparticles) were characterized and tested for determining the antioxidant concentration required  
294 for the 50% reduction in the DPPH and tested as able antioxidant agents to perform scavenging  
295 activities in a biological environment, evaluating the ROS scavenging capacities using the SHSY-5Y  
296 tumor cell line.

### 297 *3.1 Synthesis of HytOle*

298 Procopio et al. developed a protocol for the synthesis of lipophilic hydroxytyrosol fatty acid  
299 conjugates using lanthanoid salts as Lewis acid catalysts (Procopio et al. 2009). The method involved  
300 the use of erbium triflate in anhydrous conditions and a solvent not environmentally sustainable as  
301 acetonitrile. The synthetic method proposed in the present work was more convenient using 2-  
302 MeTHF as a green solvent in non-anhydrous conditions with still excellent yield, selectivity of the  
303 desired product (93% yield) and an easy work-up process. The HytOle was characterized using <sup>1</sup>H-  
304 NMR and <sup>13</sup>C-NMR spectroscopy (see Supporting Information).

### 305 *3.2 Particle size, zeta potential and stability of SLN-HtyrOle based.*

306 The hydrodynamic diameter and zeta potential were detected by DLS.

307 Please Insert the Table 1 here

308 As shown in Table 1, the mean particle size of HtyOLE conjugate nanoparticles increased after  
309 oleuropein and oleuropein derivatives incorporation, indicating the successful encapsulation of OPs  
310 inside the HtyOle nanoparticle.

311 The SLN-HtyOle particle size was 141 nm, and the PDI value was 0.177. The addition of oleuropein,  
312 its suitably synthesized aglycone and hydroxytyrosol increased ( $p < 0.05$ ) particle size of the formed  
313 nanoparticles. The measured PDI of SLNs was in all cases approximately 0.2, demonstrating the  
314 excellent dispersion of prepared nanoparticles.

315 The SLNs were stable at 4 °C over a period of 60 days, unchanging mean particle size and PDI at  
316 day 1, 30 and 60 (Table 1, gray entries). When the same SLNs were stored at 25 °C, the mean particle  
317 size increased (Table 1, white entries) compared to samples stored at 4-8 °C.

### 318 *3.3 Encapsulation efficiencies, loading capacity and in vitro release of OL, 3,4-DHPEA-EA and Hty*

319 The encapsulation efficiencies (EE) and loading capacity (LC) of SLN-HtyOle based containing OL,  
320 3,4-DHPEA-EA and Hty reported in Table 2.

321 The loading efficiency of all formulations was evaluated through HPLC by comparison with a  
322 standard curve obtained using OL, 3,4-DHPEA-EA and Hty respectively solution in methanol at  
323 known PC concentrations (Table 2). The results showed that both formulations have a loading  
324 efficiency of 99.25%, 98.81% and 99.21% for SLN-HtyOle-OL, SLN-HtyOle-3,4-DHPEA-EA and  
325 SLN-HtyOle-Hty ( $n = 3$ ) respectively. The PC concentrations were used as an abscissa and the  
326 absorbance was used as the ordinate for standard curve construction (See Supporting Information).

327 Please Insert the Table 2 here

328 As shown in Table 2, the EE of PCs in SLN-HtyOle was very high and the SLN-HtyOle-OL and  
329 SLN-HtyOle-Hty showed the best encapsulation efficiency. The PCs loading amount were  
330 approximately 6 %.

331 Release curves (Figure 2) showed that free PCs were released rapidly while the encapsulated PCs  
332 tended to be released slowly showing better sustained-release properties. Particularly interesting  
333 were the results obtained for the SLN-HtyOle-Hty.

334 Please Insert the Figure 2 here

335 The excellent sustained-release behavior might increase the bioavailability of PCs *in vivo*.

#### 336 3.4. Antioxidant Activity measured using DPPH Assay.

337 The significant antioxidant potentials of SLNs-HtyOle based obtained were evaluated by DPPH  
338 radical scavenging assay having IC<sub>50</sub> ranging between 1.13 μM (for SLN-HtyOle-3,4-DHPEA-EA)  
339 and 26.19 μM (for OL) (Table 3).

340 Please Insert the Table 3 here

341 As expected, the test determining the antioxidant concentration required a 50% reduction in the  
342 DPPH as it was performed in an organic environment (namely, in MeOH) and it has been observed  
343 an IC<sub>50</sub> at a concentration 10 times lower for formulated nanoparticles (Table 3, entries 2, 3 and 4)  
344 than the corresponding free polyphenol (Table 3, entries 5, 6 and 7). Particularly interesting was the  
345 data obtained for SLN-HtyOle which showed an IC<sub>50</sub> value equal to 6.32 μM (Table 3, entry 1)  
346 compared to the value of non-conjugated hydroxytyrosol and not in the form of nanoparticles which  
347 showed an IC<sub>50</sub> value equal to 13.05 μM (Table 3, entry 7). Also, Hty itself has an even lower IC<sub>50</sub>  
348 value (3.22 μM) if it is encapsulated (Table 3, entry 4). The encapsulated OL (Table 2, entry 2)  
349 showed a value almost fourteen times lower (1.92 μM) than the free OL (Table 2, entry 5) which  
350 showed an IC<sub>50</sub> value equal to 26.19 μM. Even more significant were the differences in the results  
351 regarding 3,4-DHPEA-EA. The encapsulated aglycone (Table 2, entry 3) showed an IC<sub>50</sub> value  
352 twenty-two times lower (1.13 μM) than the same free aglycone that showed an IC<sub>50</sub> value equal to  
353 25.23 μM (Table 2, entry 6).



### 354 3.5 *In vitro* antioxidant activity determination

355 For the evaluation of the antioxidant activity of OPs, a combination of several chemical and cell  
356 culture assays are available. Cell culture assays are used to determine the physiological functions and  
357 to measure cytotoxic effects in response to oxidative stress or cytoprotection by antioxidants (Gülden,  
358 Jess, Kammann, Maser, & Seibert, 2010). Thus, to evaluate the protective effects of the formulated  
359 nanoparticles in a cellular system (insulted by a pro-oxidant agent), we employed human neuron-like  
360 cells SH-SY5Y as an *in vitro* model. These cells elicit a functional response like human neurons, such  
361 as outgrow neurites and undergo morphological changes when challenged by oxidative stress *in vitro*  
362 (Rabelo et al., 2012).

363 In a recent review, R Huang et al. (Huang et al, 2021) clearly showed that ROS play a dual role in the  
364 initiation, development, suppression, and treatment of cancer. Furthermore, ROS inhibition is a  
365 practical test useful for determining whether an antioxidant agent is able to perform its scavenging  
366 activities in a biological environment, thus correlating the results with the bioavailability of the tested  
367 compounds. To comprehend whether the increased bioavailability of the encapsulated PCs could  
368 reflect stronger antioxidant activities in the cells than the free PCs, we evaluated the ROS scavenging  
369 capabilities of the synthesized nanoparticles by determining their ROS levels in a biological  
370 environment using the SHSY-5Y tumor cell line. (Figure 3). After exposed SHSY-5Y cells to  
371 extracellular ROS attack by 6-OHDP (6-hydroxydopamine) and pretreated with different  
372 concentrations of free PCs (OL, Hty, 3,4-DHPEA-EA) and the respective SLN-HtyOle based  
373 nanoparticles with and without PCs (SLN-HtyOle-OL, SLN-HtyOle-Hty, SLN-HtyOle-3,4-DHPEA-  
374 EA an SLN-HtyOle) (0.1, 0.05, 0.01 and 0.005  $\mu\text{M}$ ), % ROS formation was determined by the  
375 previously described fluorescence method. In the presence of SLN-HtyOle based nanoparticles, ROS  
376 generation was significantly reduced, and a 50% reduction in ROS formation was observed at only  
377 0.01  $\mu\text{M}$ . Otherwise, in the presence of free PCs ROS generation was significantly reduced, and a  
378 50% reduction in ROS formation was observed at 0.05  $\mu\text{M}$ . Treating SHSY-5Y cells with formulated  
379 nanoparticle PC free (SLN-HtyOle), a 25.13% reduction in ROS formation was observed at the same

380 concentration (0.05  $\mu\text{M}$ ) and ~19% ROS formation with formulated nanoparticles containing OL,  
381 Hty and 3,4-DHPEA-EA (SLN-HtyOle-OL, SLN-HtyOle-Hty, SLN-HtyOle-3,4-DHPEA-EA  
382 respectively) Cell proliferation tests were performed on the SH-SY5Y cells using an SRB assay (Figure  
383 4). The Figure 4 (SRB Assay) showed that using 0.1  $\mu\text{M}$  of all formulations the percentage of control  
384 cell growth is almost 100%.

385 Please Insert the Figure 3 here

386 Please Insert the Figure 4 here

387 50% reduction in ROS formation was observed at only 0.01  $\mu\text{M}$  when the cells were pretreated  
388 with formulated nanoparticles. This demonstrates the hypothesis of the correlation between cellular  
389 bioavailability and antioxidant activity.

#### 390 **4. Conclusions**

391 In conclusion, SLN-HtyOle and SLN-HtyOle-OL(Hty)(3,4-DHPEA-EA) were synthesized and  
392 characterized for loading efficiency, size and antioxidant activity.

393 The results showed that both formulations have a great loading efficiency and dimensions over the  
394 range of 141-173 nm. Furthermore, the present paper proposes a new, simple and sustainable method  
395 for the synthesis of HtyOle and new nanoparticles HtyOle based containing OL, Hty and 3,4-DHPEA-  
396 EA. The obtained nanoformulations showed greater antioxidant activity and an excellent sustained-  
397 release. . In particular, this paper clearly demonstrated that the increased bioavailability of  
398 polyphenolic compounds as oleuropein derivatives is responsible for the compounds' augmented  
399 radical-scavenging capacity in an organic medium as well as in a biological environment. The  
400 encapsulated OPs slowly released and showed a much lower ROS formation value than the respective  
401 free OPs. This demonstrates the effectiveness of the proposed nanoformulations which could be used  
402 in the future on *in vivo* models.

403

404 **Aknowledgements**

405 This work was supported by the National Project ‘‘Ricerca e Innovazione per l’Olivicoltura  
406 Meridionale (RIOM)’’ from the Italian Ministry of Agriculture and by the APQ-RAC project  
407 QUASIORA from Calabrian Regional government.

408

409 **Appendix A.** Supplementary data associated with this article can be found, in the online version, at  
410 [http//.....](http://.....)

411 **References**

412 Alcaide- Hidalgo, J. M. , Romero, M., Duarte, J., López- Huertas, E. (2020). Antihypertensive  
413 Effects of Virgin Olive Oil (Unfiltered) Low Molecular Weight Peptides with ACE Inhibitory  
414 Activity in Spontaneously Hypertensive Rats. *Nutrients*, 12, 271

415 Benincasa, C., La Torre, C., Plastina, P., Fazio, A., Perri, E., Caroleo, M. C., Gallelli, L., Cannataro,  
416 R., Cione, E. (2020). Hydroxytyrosyl Oleate: Improved Extraction Procedure from Olive Oil and  
417 By-Products, and In Vitro Antioxidant and Skin Regenerative Properties. *Antioxidants*, 9, 998-  
418 1008

419 Campolo, M., Di Paola, R., Impellizzeri, D., Crupi, R., Morittu, V. M., Procopio, A., Perri, E., Britti,  
420 D., Peli, A., Esposito, E., Cuzzocrea, S. (2013). Effects of a polyphenol present in olive  
421 oil, oleuropein aglycone, in a murine model of intestinal ischemia/reperfusion injury. *Journal*  
422 *of Leukocyte Biology*, 93, 277-287

423 Cavaca, L. A. S., Afonso, C. A. M. (2018) Oleuropein: A Valuable Bio-Renewable Synthetic  
424 Building Block. *European Journal of Organic Chemistry*, 5, 581-589

425 Costanzo, P., Bonacci, S., Cariati, L., Nardi, M., Oliverio, M., Procopio, A. (2017) Simple and  
426 Efficient Sustainable Semi-synthesis of oleacein [2-(3,4-hydroxyphenyl) ethyl (3S,4E)-4-  
427 formyl-3-(2-oxoethyl)hex-4-enoate] as potential additive for edible oils. *Food Chemistry*, 245,  
428 410-414.

429 D'Archivio, M., Filesi, C., Vari, R., Scazzocchio, B., Masella, R. (2010) Bioavailability of the OPs:  
430 Status and Controversies. *International Journal of Molecular Sciences*, 11, 1321-1342

431 Ekambaram, P.; Sathali, A.A.H.; Priyanka, K. (2012) Solid lipid nanoparticles: A review. *Sci. Revs.*  
432 *Chem. Commun.*, 2, 80–102.

433 Giada, J., Oliverio, M., Bellizzi, D., Gallo Cantafio, M. E., Grillone, K., Passarino, G., Colica, C.,  
434 Nardi, M., Rossi, M., Procopio, A., Tagliaferri, P., Tassone, P., Amodio, N. (2019), "Anti-  
435 tumor Activity and Epigenetic Impact of the Polyphenol Oleacein in Multiple  
436 Myeloma" *Cancers* 11, 7: 990.

437 Gülden, M., Jess, A., Kammann, J., Maser, E., & Seibert, H. (2010). Cytotoxic potency of H<sub>2</sub>O<sub>2</sub> in  
438 cell cultures: Impact of cell concentration and exposure time. *Free Radical Biology &*  
439 *Medicine*, 49, 1298–1305.

440 Guo, L., Sun, Q., Gong, S., Bi, X., Jiang, W., Xue, W., Fei, P. (2019), Antimicrobial Activity and  
441 Action Approach of the Olive Oil Polyphenol Extract Against *Listeria monocytogenes*.  
442 *Frontiers in Microbiology*, 10, 1586

443 Hare, J.I., Lammers, T., Ashford, M.B., Puri, S., Storm, G., Barry, S.T. (2017) Challenges and  
444 strategies in anti-cancer nanomedicine development: an industry perspective. *Advanced*  
445 *Drug Delivery Reviews*, 108, 25–38.

446 Hornedo-Ortega, R.; Cerezo, A. B.; de Pablos, R M.; Krisa, S.; Richard, T.; García-Parrilla, M. C.;  
447 Troncoso, A: M. (2018) Phenolic Compounds Characteristic of the Mediterranean Diet in  
448 Mitigating Microglia-Mediated Neuroinflammation. *Frontiers in Cellular Neuroscience*, 12,  
449 Article 373

450 Karantonis, H. C., Antonopoulou, S., Perrea, D. N., Sokolis, D. P., Theocharis, S. E., Kavantzias, N.,  
451 Iliopoulos, D. G., Constantinos A. Demopoulos, (2006) In vivo antiatherogenic properties of

452 olive oil and its constituent lipid classes in hyperlipidemic rabbits. *Nutrition, Metabolism and*  
453 *Cardiovascular Diseases*, 16, 3, 174-185

454 Kiss, A.K., Mańk, M., Melzig, M.F. (2008). Dual inhibition of metallopeptidases ACE and NEP by  
455 extracts, and iridoids from *Ligustrum vulgare* L. *Journal of Ethnopharmacology*, 120, 220-  
456 225.

457 Impellizzeri, D., Esposito, E., Mazzon, E., Paterniti, I., Di Paola, R., Bramanti, P., Morittu, V.M.,  
458 Procopio, A., Britti, D., Cuzzocrea, S. (2011) The effects of oleuropein aglycone, an olive  
459 oil compound, in a mouse model of carrageenan-induced pleurisy. *Clinical Nutrition*, 30,  
460 533–540.

461 Mancuso, S., Costanzo, P., Bonacci, S., Nardi, M., Oliverio, M., Procopio, A.(2021) Green  
462 Semisynthetic Cascade to Ligstroside, Ligstroside Aglycone, and Oleocanthal ACS  
463 *Sustainable Chemistry & Engineering*, 9, 12614–12622

464 Mazzei, R., Piacentini, E., Nardi, M., Poerio, T., Bazzarelli, F., Procopio, A., Di Gioia, M.L., Rizza,  
465 P., Ceraldi, R., Morelli, C., Giorno, L., Pellegrino, M. (2020) Production of Plant-Derived  
466 Oleuropein Aglycone by a Combined Membrane Process and Evaluation of Its Breast  
467 Anticancer Properties. *Frontiers in Bioengineering and Biotechnology* 8; 908.

468 Nardi, M, Sindona, G, Costanzo, P, Oliverio, M, Procopio, A (2015) Eco-friendly stereoselective  
469 reduction of  $\alpha,\beta$ -unsaturated carbonyl compounds by  $\text{Er}(\text{OTf})_3/\text{NaBH}_4$  in 2-MeTHF.  
470 *Tetrahedron*, 71:1132-1135

471 Nardi, M., Herrera Cano, N., De Nino, A., Di Gioia, M.L., Maiuolo, L., Oliverio, M., Santiago, A.,  
472 Sorrentino, D., Procopio, A. (2017) An eco-friendly tandem tosylation/Ferrier N-glycosylation  
473 of amines catalyzed by  $\text{Er}(\text{OTf})_3$  in 2-MeTHF. *Tetrahedron Letters*, 58, 18: 1721–1726

474 Nardi, M., Bonacci, S., Cariati, L., Costanzo, P., Oliverio, M., Sindona, G., Procopio, A. (2017)  
475 Synthesis and antioxidant evaluation of lipophilic oleuropein aglycone derivatives. *Food &*  
476 *Function*, 8, 4684-4692.

477 Nardi, M., Bonacci, S., De Luca, G., Maiuolo, J., Oliverio, M., Sindona, G. Procopio, A. (2014).  
478 Biomimetic synthesis and antioxidant evaluation of 3,4-DHPEA-EDA [2-(3,4- hydroxyphenyl)  
479 ethyl (3S,4E)-4-formyl-3-(2-oxoethyl)hex-4-enoate]. *Food Chemistry*, 162, 89-93.

480 Nardi, M., Herrera Cano, N., De Nino, A., Di Gioia, M.L., Maiuolo, L., Oliverio, M., Santiago, A.,  
481 Sorrentino, D., Procopio, A. (2017) An eco-friendly tandem tosylation/Ferrier *N*-  
482 glycosylation of amines catalyzed by Er(OTf)<sub>3</sub> in 2-MeTHF. *Tetrahedron Letters*, 58, 18:  
483 1721-1726

484 Nardi, M., Baldelli, S., Ciriolo M.R., Costanzo, P., Procopio, A., Colica, C. (2020) Oleuropein  
485 Aglycone Peracetylated (3,4-DHPEA-EA(P)) Attenuates H<sub>2</sub>O<sub>2</sub>-Mediated Cytotoxicity in  
486 C2C12 Myocytes via Inactivation of p-JNK/p-c-Jun Signaling Pathway. *Molecules*, 25(22),  
487 5472

488 Nassimi, M., Schleh, C., Lauenstein, H.D., Hussein, R., Hoymann, H.G., Koch, W., Pohlmann, G.,  
489 Krug, N., Sewald, K., Rittinghausen, S., Braun, A., Müller-Goymann, C. (2010) A  
490 toxicological evaluation of inhaled solid lipid nanoparticles used as a potential drug delivery  
491 system for the lung *European Journal of Pharmaceutics and Biopharmaceutics*, 7, 107–116

492 Oh, W. Y., Shahidi, F. (2017) Lipophilization of Resveratrol and Effects on Antioxidant Activities.  
493 *Journal Agricultural Food Chemistry*. 65, 39, 8617–8625

494 Okonko, I. O., Adeola, O. T., Aloysius, F. E., Damilola, A. O., Adewale, O. A. (2009) Utilization  
495 of food wastes for sustainable development. *Electronic Journal of Environmental,*  
496 *Agricultural and Food Chemistry*, 8 (4), 263-286.

497 Pardeike, J., Hommoss, A., Müller, R.H. (2009) Lipid nanoparticles (SLN, NLC) in cosmetic and  
498 pharmaceutical dermal products. *International Journal of Pharmaceutics*, 366, 170–184

499 Petkar, K.C., Chavhan, S., Kunda, N., Saleem, I., Somavarapu, S., Taylor, K.M.G., Sawant, K.K.  
500 (2018) Development of Novel Octanoyl Chitosan Nanoparticles for Improved Rifampicin  
501 Pulmonary Delivery: Optimization by Factorial Design. *American Association of*  
502 *Pharmaceutical Scientists*, 19, 4, 1758–1772

503 Plastina, P., Benincasa, C., Perri, E., Fazio, A., Augimeri, G., Poland, M., Witkamp, R., Meijerink J.  
504 (2019). Identification of hydroxytyrosyl oleate, a derivative of hydroxytyrosol with anti-  
505 inflammatory properties, in olive oil by-products. *Food Chemistry*. 279 105–113

506 Procopio, A., Alcaro, S., Nardi, M., Oliverio, M., Ortuso, F., Sacchetta, P., et al. (2009). Synthesis,  
507 biological evaluation, and molecular modeling of oleuropein and its semisynthetic derivatives as  
508 cyclooxygenase inhibitors. *Journal of Agricultural and Food Chemistry*, 57, 11161–11167.

509 Procopio, A., Celia, C., Nardi, M., Oliverio, M., Paolino, D., Sindona, G. (2011) Lipophilic  
510 Hydroxytyrosol Esters: Fatty Acid Conjugates for Potential Topical Administration. *Journal*  
511 *Natural Product*, 74, 11, 2377–2381

512 Procopio, A., Celia, C., Nardi, M., Oliverio, M., Paolino, D., Sindona, G. (2011). Lipophilic  
513 Hydroxytyrosol Esters: Fatty Acid Conjugates for Potential Topical Administration. *Journal*  
514 *Natural Product*, 74, 11, 2377–2381

515 Rabelo, T. K., Zeidán-Chuliá, F., Vasques, L. M., Santos, J. P. A., Rocha, R. F., Pasquali, M. A. B.,  
516 Gelain, D. P. (2012). Redox characterization of usnic acid and its cytotoxic effect on human  
517 neuron-like cells (SH-SY5Y). *Toxicology in Vitro*, 26, 304–314.

518 Rizzo, M., Ventrice, D., Giannetto, F., Cirinnà, S., Santagati, N.A., Procopio, A., Mollace, V.,  
519 Muscoli, C. (2017), Antioxidant activity of oleuropein and semisynthetic acetyl-derivatives  
520 determined by measuring malondialdehyde in rat brain. *Journal of Pharmacy and Pharmacology*,  
521 69(11):1502-151

522 Scioli Montoto, S., Muraca, G., Ruiz, M.E. (2020) Solid Lipid Nanoparticles for Drug Delivery:  
523 Pharmacological and Biopharmaceutical Aspects. *Frontiers in Molecular Biosciences.*, 7:  
524 587997

525 Sindona, G., Caruso, A., Cozza, A., Fiorentini, S., Lorusso, B., Marini, E., Nardi, M., Procopio, A.,  
526 Zicari, S. (2012). Anti-Inflammatory Effect of 3,4-DHPEA-EDA [2-(3,4 -Hydroxyphenyl)  
527 ethyl (3S, 4E)- 4-Formyl-3-(2-Oxoethyl)Hex-4-Enoate] on Primary Human Vascular  
528 Endothelial Cells. *Current Medicinal Chemistry*, 19, 23, 4006 – 4013

529 Skehan, P., Storeng, R., Scudiero, D., Monks, A.; McMahon, J.; Vistica, D.; Warren, J. T.; Heidi  
530 Bokesch, H.; Kenney, S.; Boyd, M. R. (1990) New colorimetric cytotoxicity assay for  
531 anticancer-drug screening. *Journal of National Cancer Institute*, 82, 1107–1112.

532 Tapeinos, C., Battaglini, M., Ciofani, G. (2017) Advances in the Design of Solid Lipid  
533 Nanoparticles and Nanostructured Lipid Carriers for Targeting Brain Diseases. *Journal of*  
534 *Controlled Release*, 264, 306–332.

535 Vichai, V., Kirtikara, K. (2006) Sulforhodamine B colorimetric assay for cytotoxicity screening.  
536 *Nature protocols*, 1, 1112– 1116

537 Visioli, F.; Bellomo, G.; Galli, C. (1998). Free Radical-Scavenging Properties of Olive Oil OPs.  
538 *Biochemical and Biophysical Research Communications*, 247, 60–64.

539 Wang, J., Sun, D., Huang, L., Wang, S., Jin, Y. (2021) Targeting Reactive Oxygen Species Capacity  
540 of Tumor Cells with Repurposed Drug as an Anticancer Therapy, *Oxidative Medicine and*  
541 *Cellular Longevity* Article ID 8532940, 17.

542 Xie, J., Schaich, K. M. (2014). Re-evaluation of the 2,2-Diphenyl-1-picrylhydrazyl Free Radical  
543 (DPPH) Assay for Antioxidant Activity. *Journal Agricultural Food Chemistry*, 62,  
544 4251–4260



545 Yang, B., Dong, Y., Wang, F., Zhang, Y. (2020) Nanoformulations to Enhance the Bioavailability  
546 and Physiological Functions of Polyphenols. *Molecules*, 25, 4613

547 Zihua, L., Yan, Z., Yuefei, W., Xianqiang Y., Baolu, Z. (2012) Protective effect of theaflavins on  
548 neuron against 6-hydroxydopamine-induced apoptosis in SH-SY5Y cells. *Journal of Clinical*  
549 *Biochemistry and Nutrition*, 50(2), 133–138.

550 Zupančić, S., Kocbek, P., Zariwala, M.G., Renshaw, D., Gul, M.O., Elsaid, Z., Taylor, K.M.,  
551 Somavarapu, S. (2014) Design and development of novel mitochondrial targeted nanocarriers,  
552 DQAsomes for curcumin inhalation. *Molecular Pharmaceutics*, 11, 7, 2334–2345.

553

554

555

556

557

558

559

560

561

562

563

564

565

566

567

568

569

570 **Figure and Table Captions**

571 **Figure 1.** Molecular structure of hydroxytyrosol oleate, Oleuropein, 3,4-DHPEA-EA and  
572 Hydroxytyrosol

573 **Figure 2.** In vitro release profiles of SLN-HtyOle-OL, SLN-HtyOle-3,4-DHPEA-EA, SLN-HtyOle-  
574 Hty and PCs free. Data expressed as means  $\pm$  SD ( $n = 3$ ). \*\*\*  $p < 0.001$  versus corresponding free  
575 drugs

576 **Figure 3.** ROS formation: SHSY-5Y cells were exposed to the extracellular ROS attack by 6-OHDP  
577 25  $\mu$ M (and pretreated with free PCs as OL, Hty and 3,4-DHPEA-EA and the correspondents  
578 nanoparticles encapsulated in SLN-HtyOle to concentrations 0.1, 0.05 and 0.01 and 0.005  $\mu$ M). Data  
579 expressed as means  $\pm$  SD of three independent observations. \*\*\* $p < 0.001$  versus SLN-HtyOle; ###  
580  $p < 0.001$  versus Control.

581 **Figure 4.** SRB assay: assay SRB for determination % of control cell growth. Data expressed as means  
582  $\pm$  SD of three independent observations. \*\*\* $p < 0.001$  versus SLN-HtyOle; ###  $p < 0.001$  versus  
583 Control. \*\* $p < 0.01$  versus SLN-HtyOle; §  $p < 0.1$  versus Control.

584 **Table 1.** Size distribution and surface charge of SLN-HtyOle, SLN-HtyOle-OL, SLN-HtyOle-3,4-  
585 DHPEA-EA, SLN-HtyOle-Hty stored at 25 °C and 4 °C at day 1, 30 and 60.<sup>a</sup>

586 **Table 2.** Drug loading and drug entrapment efficiencies of SLN-HtyOle-OL , SLN-HtyOle-3,4-  
587 DHPEA-EA and SLN-HtyOle-Hty ( $n = 3$ ).

588

589

590

591

592

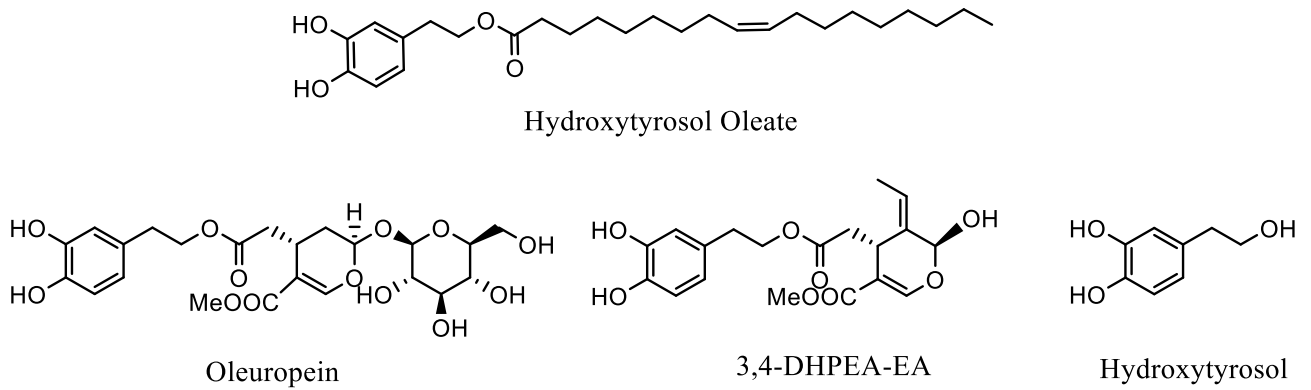
593

594

595

596 **Figure 1**

597

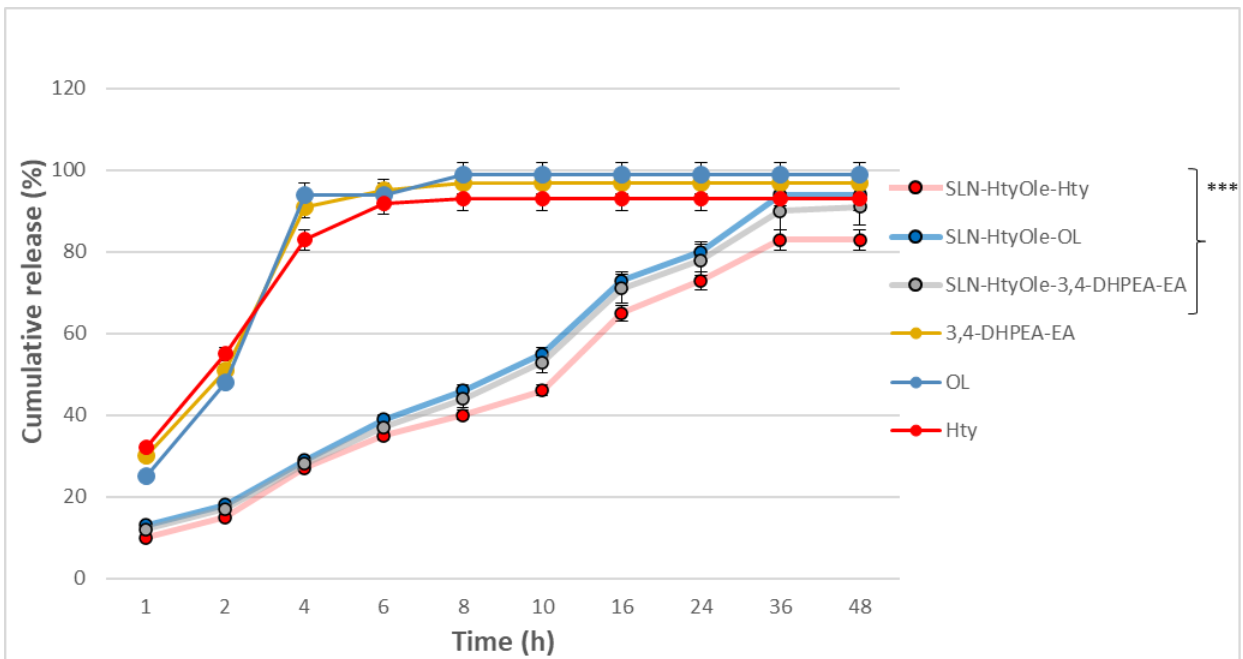


598

599

600

601 **Figure 2**



602

603

604

605

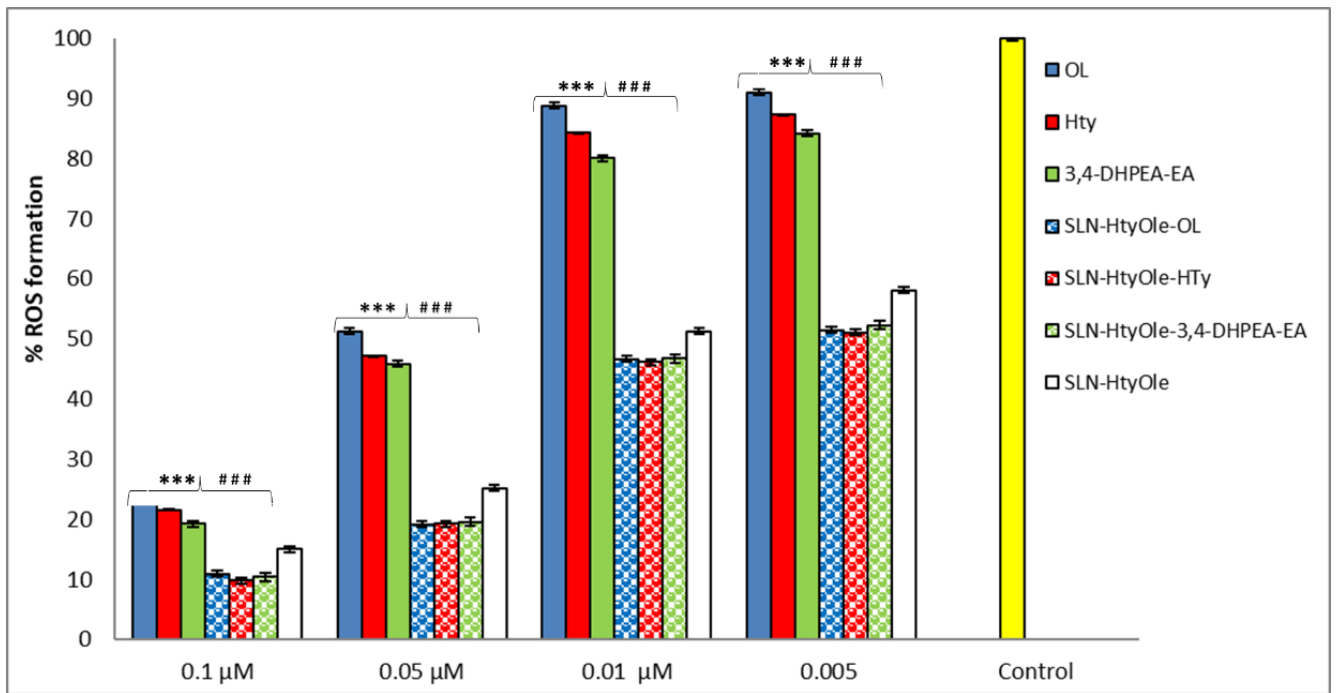
606

607

608

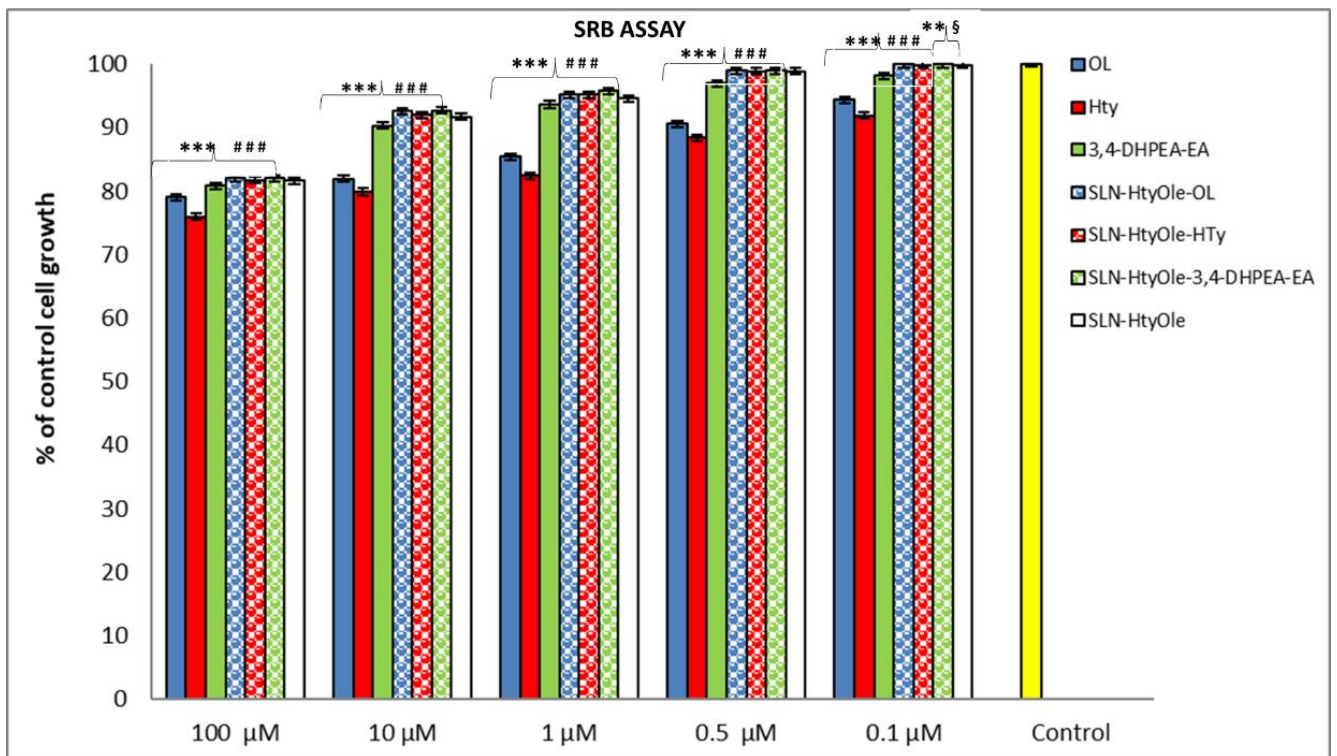
609

610 **Figure 3**



611

612 **Figure 4**



613

614

615

616

**Table 1.**

| Storage condition      | SLN-HtyOle       | SLN-HtyOle-OL    | SLN-HtyOle-3,4-DHPEA-EA | SLN-HtyOle-Hty   |
|------------------------|------------------|------------------|-------------------------|------------------|
| <b>Day 1 (Initial)</b> |                  |                  |                         |                  |
| Particle size (nm)     | 141.3 ± 0.139    | 147.5 ± 0.153    | 173.4 ± 0.261           | 162.8 ± 0.764    |
| PDI                    | 0.177 ± 0.017    | 0.181 ± 0.027    | 0.229 ± 0.018           | 0.233 ± 0.032    |
| Zeta potential (mV)    | -41.3 ± 0.349    | -10.3 ± 0.599    | -23.7 ± 0.643           | -28.6 ± 0.586    |
| <b>Day 30 at 4 °C</b>  |                  |                  |                         |                  |
| Particle size (nm)     | ***153.3 ± 0.220 | ***160.7 ± 1.051 | ***179.1 ± 0.218        | ***170.0 ± 0.534 |
| PDI                    | 0.170 ± 0.012    | 0.183 ± 0.011    | 0.230 ± 0.018           | 0.235 ± 0.022    |
| Zeta potential (mV)    | -41.4 ± 0.151    | -10.1 ± 0.112    | -23.1 ± 0.206           | -28.7 ± 0.570    |
| <b>Day 30 at 25 °C</b> |                  |                  |                         |                  |
| Particle size (nm)     | ***265.0 ± 0.120 | ***272.3 ± 1.140 | ***297.2 ± 0.204        | ***187.8 ± 0.214 |
| PDI                    | 0.191 ± 0.012    | 0.193 ± 0.036    | 0.237 ± 0.074           | 0.240 ± 0.030    |
| Zeta potential (mV)    | -43.4 ± 0.254    | -12.7 ± 0.312    | -25.01 ± 0.276          | -29.8 ± 0.554    |
| <b>Day 60 at 4 °C</b>  |                  |                  |                         |                  |
| Particle size (nm)     | ***152.9 ± 0.200 | ***160.9 ± 0.951 | ***178.9 ± 0.198        | ***170.6 ± 0.333 |
| PDI                    | 0.171 ± 0.012    | 0.184 ± 0.031    | 0.230 ± 0.018           | 0.235 ± 0.022    |
| Zeta potential (mV)    | -41.4 ± 0.151    | -10.1 ± 0.112    | -23.1 ± 0.206           | -28.7 ± 0.570    |
| <b>Day 60 at 25 °C</b> |                  |                  |                         |                  |
| Particle size (nm)     | ***268.2 ± 1.016 | ***278.5 ± 1.034 | ***298.1 ± 1.126        | ***190.8 ± 0.654 |
| PDI                    | 0.188 ± 0.017    | 0.117 ± 0.043    | 0.225 ± 0.011           | 0.250 ± 0.073    |
| Zeta potential (mV)    | -43.99 ± 0.201   | -12.9 ± 0.134    | -26.19 ± 0.161          | -30.2 ± 0.750    |

<sup>a</sup>Each formulation was prepared at least six times and measurements were taken in triplicate for each sample. (\*\*\*  $p < 0.001$  versus Day 1).

**Table 2**

|                         | <b>Entrapment efficiency</b> | <b>LC</b>             |
|-------------------------|------------------------------|-----------------------|
|                         | <b>(Mean %, ± SD)</b>        | <b>(Mean %, ± SD)</b> |
| SLN-HtyOle-OL           | 99.248 ± 0.327               | 6.10 ± 0.04           |
| SLN-HtyOle-3,4-DHPEA-EA | 98.815 ± 0.187               | 6.01 ± 0.05           |
| SLN-HtyOle-Hty          | 99.212 ± 0.521               | 6.08 ± 0.03           |

624

**Table 3.** Free radical-scavenging activities measured using the DPPH assay.<sup>a</sup>

| <b>Entry</b> | <b>Compound</b>            | <b>IC<sub>50</sub>±SD [µM]</b> |
|--------------|----------------------------|--------------------------------|
| 1            | SLN-HtyOle                 | 6.32±0.01                      |
| 2            | ***SLN-HtyOle-OL           | 1.92±0.02                      |
| 3            | ***SLN-HtyOle-3,4-DHPEA-EA | 1.13±0.05                      |
| 4            | ***SLN-HtyOle-Hty          | 2.67±0.05                      |
| 5            | ***OL                      | 26.19±0.24                     |
| 6            | ***3,4-DHPEA-EA            | 25.23±1.06                     |
| 7            | ***Hty                     | 13.05±0.15                     |

<sup>a</sup>Data are expressed as the means ± SD of three independent observations. \*\*\* $p < 0.001$  versus SLN-HtyOle).

625

Reviewers' comments:

**Reviewer #1:**

1. Not all the materials used in the study are listed. Please declare the purity of Hydroxytyrosol

**A:** In accordance with the Reviewer's suggestion, in the line 117 we reported "Hydroxytyrosol was purchased from TCI AMERICA (Purity: >98.0% (GC))"

2. Filtration is not the correct method to remove the free drug for the determination of EE. Dialysis method under cold condition should be used.

**A:** It has been a mistake reporting the filtration type. We purified the sample by means of Amicon® Ultracentrifugal Filters (cut-off 10 kDa, 4000 rpm for 60 min). In accordance with the Reviewer's suggestion, we reported the correct used method.

3. What is the surface area of the dialysis membrane used in the release study? The more the area, faster/higher will be release. Please define the area of the membrane exposed to the formulation.

**A:** In accordance with the Reviewer's suggestion, in the line 204 we reported "a cellulose acetate dialysis tube (12 kDa, diameter 16 mm, 2ml/cm, A=29,14 cm<sup>2</sup>) (Spectra/Pro, Spectrum Lab, Breda, Netherlands)"

4. What is the rationale for dispersing the formulation in 75mg/1 ml of the buffer?

**A:** The saturated solubility of Hydroxytyrosol in the water is 5gr/100ml (50mg/ml). The solubility of oleuropeine (less soluble) in the water is 0,73mg/ml. In the formulations it is 10mg of the drugs in the 75mg. However, in order to operate under sink conditions, the investigation of drug release profiles was performed using 1 ml of solution buffer containing 10 mg of the drug, placed into dialysis bags moved into beaker (100 ml of the release medium).

5. Why were cell uptake studies not conducted? Current cell culture-based assays appear to be inadequate make strong conclusions?

**A:** The authors' goal was to test the antioxidant activities of the new nanoformulations using neuroblastoma SH-SY5Y cell line. From these results we could start to subsequently carry out cell uptake studies of promising neuroprotective nanocarrier delivery system.

6. Why did authors not select accelerated conditions? Current studies provide only 4 and 25 deg C?

**A:** In this work, our aim is to demonstrate the nanoformulations stability at storage temperatures and room temperature even after 60 days. Therefore, we did not consider the use of further drastic conditions appropriate.

## Reviewer #2:

This paper deals with the preparation of a new carrier-free drug system using hydroxytyrosol oleate as solid lipid for the synthesis of nanoparticles containing phenolic compounds (PCs) as OL, 3,4-DHPEA-EA and Htyr. The synthesis of hydroxytyrosol oleate was also described. The aim of this work was to evaluate the bioavailability of the encapsulated polyphenolic compounds using hydroxytyrosyl oleate-based solid lipid nanoparticles, their antioxidant activity and ROS formation on neuroblastoma SH-SY5Y cell line. A combination of techniques was used. However, there are some major issues to be addressed before its publication.

1. The article needs extensive English editing. Expression and syntax must be improved throughout the manuscript. Also, there are plenty of typos in the text that should be corrected.

**A:** In accordance with the Reviewer's suggestion, we reviewed the article making the appropriate corrections.

2. A review of the highlights is recommended.

**A:** In accordance with the Reviewer's suggestion, we reviewed the highlights.

3. The use of extensive sentences should be avoided.

**A:** In accordance with the Reviewer's suggestion, we have reduced the length of the sentences

4. Line 126: "1 mol % of Er(OTf)<sub>3</sub> (0.0162 mmol)". What does the % refer to? Present just the mmol.

**A:** In accordance with the Reviewer's suggestion, we reported just mmol

5. Line 141: "The MW-assisted extraction of oleuropein (1)". The number 1 in the bracket to what corresponds to?

**A:** In accordance with the Reviewer's suggestion, in the line 141, we eliminate the number 1.

6. The results section should be carefully checked and re-edited as many text-flaws were found.



**A:** In accordance with the Reviewer's suggestion, we revised the results section.

7. 2-MeTHF is a biogenic solvent deriving from biomass, thus its production is indeed environmentally friendly. However, it is highly toxic when used as a solvent. Please make a comment on this, because it is a bit confusing when you describe an environmentally friendly approach for the preparation of hydroxytyrosol oleate.

**A:** 2-MeTHF is often suggested as a suitable replacement for more traditional solvents because it derives from renewable sources and is more easily recovered in reactions involving an aqueous medium, thus facilitating the recycling and reuse of this solvent. For these reasons 2-MeTHF is generally considered as a greener alternative to some traditional solvents, and its use is advocated by the ACS Green Chemistry Pharmaceutical Roundtable.

However, since to date only limited toxicological information has been disclosed on 2-MeTHF it is currently not included in the International Conference on Harmonisation (ICH) Q3C residual solvent guideline. ICH Q3C reports the Permitted Daily Exposure (PDE) values for a number of solvents which establish the limits below which there would be negligible safety concerns to patients exposed to them as residual impurities in drug products. Nevertheless, preliminary toxicological investigations suggest that exposure to 2-MeTHF is not linked to mutagenicity or genotoxicity [1]. Moreover, since 2-MeTHF is increasingly used as a solvent in the pharmaceutical industry, Parris et al. published data following the ICH methodology to enable calculation of a PDE for 2-MeTHF [2]. Their study, conducted in accordance with United Kingdom Good Laboratory Practice regulations, included multiple dose levels, an appropriate control group, a reversibility phase, and a comprehensive assessment of safety endpoints enabling the calculation of a PDE to support the safe use of 2-MeTHF in the pharmaceutical industry. Taken together these new data depict a low toxicity profile of 2-MeTHF as demonstrated in the current 3-month oral toxicity study in rats, so that should be considered appropriate to attribute a level of 1 (the lowest level, applies to agents that usually pose a minimal potential threat to laboratory workers and the environment and do not consistently cause disease in healthy adults) to safety factor F4 (no serious toxicity observed), resulting in a calculated PDE of 50 mg/day for 2-MeTHF.

[1] Toxicological Assessment of 2-Methyltetrahydrofuran and Cyclopentyl Methyl Ether in Support of Their Use in Pharmaceutical Chemical Process Development V. Antonucci John Coleman,‡ J. B. Ferry, N. Johnson, M. Mathe, J. P. Scott, J. Xu *Org. Process Res. Dev.* 2011, 15, 939-941. [dx.doi.org/10.1021/op100303c](https://doi.org/10.1021/op100303c)

[2] Calculation of a permitted daily exposure value for the solvent 2-methyltetrahydrofuran P. Parris, J. N. Duncan, A. Fleetwood, W. P. Beierschmitt *Regulatory Toxicology and pharmacology*, 2017, 87, 54-63. <http://dx.doi.org/10.1016/j.yrtph.2017.04.012>

8. Section 3.2: more concise. The authors repeat some sentences (e.g., Lines 310-312 and Lines 322-324).

**A:** In accordance with the Reviewer's suggestion, the authors deleted the repeated sentences,

9. Line 332: The authors state: "Interesting is the negative value of zeta potential for all nanoformulations". Can the authors elucidate that and explain why this is important for these nanoformulations and their application?

**A:** In accordance with the Reviewer's suggestion, the authors deleted the sentence.

10. In figure 2, the results are expressed as means  $\pm$  SD of three independent observations? Has a statistical analysis been performed?

**A.:** The authors reported the statistical analysis in the *2.9.4 Statistical analysis section*. In accordance with the Reviewer's suggestion, the authors reported in the Figure Legends, Figure 2, the sentence ". Data expressed as means  $\pm$  SD( $n = 3$ ). \*\*\*  $p < 0.001$  versus free drugs. In accordance with the Reviewer's suggestion, the authors modified figure 2

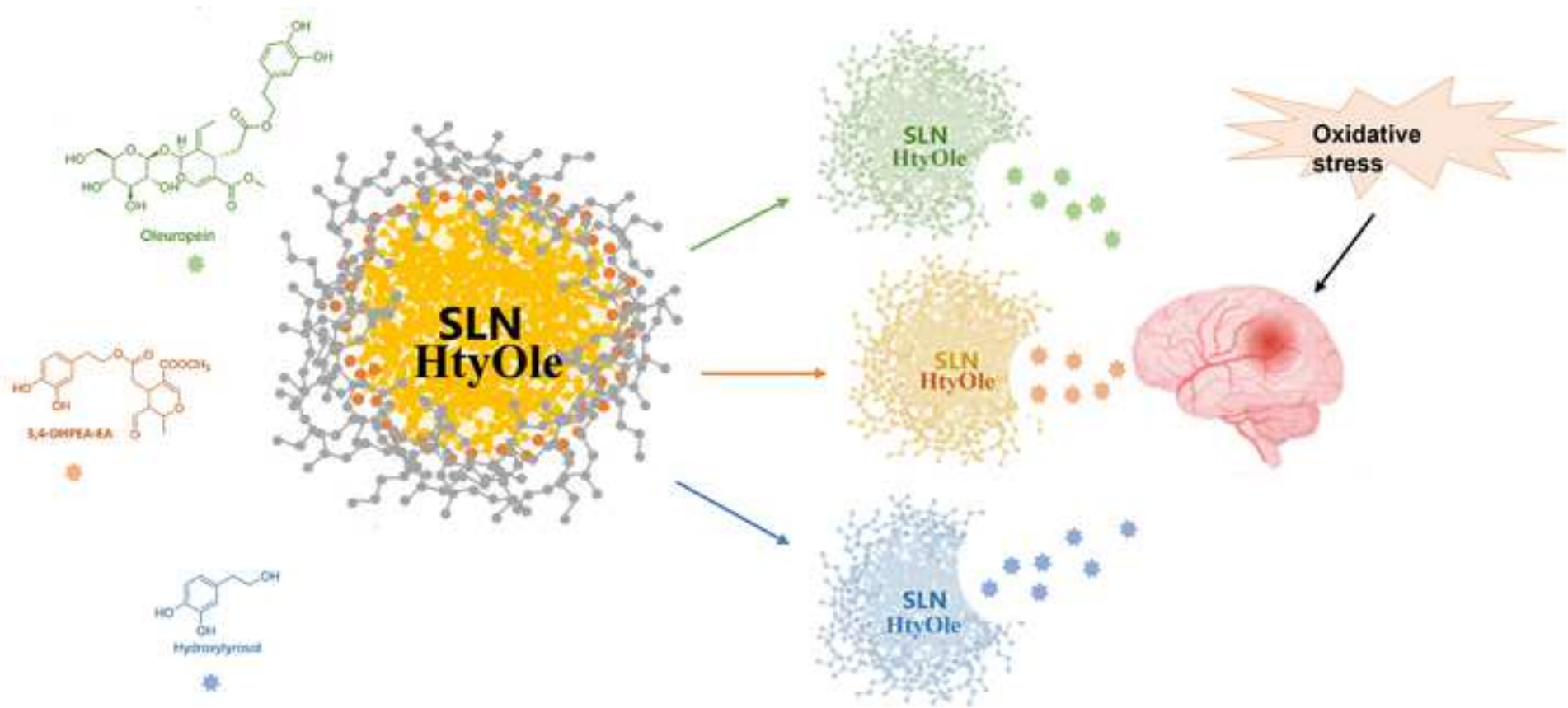
11. Table 3: How do the authors explain that the  $IC_{50}$  of free Hydroxytyrosol was the lowest among Ole derivatives whereas the  $IC_{50}$  of Hydroxytyrosol incorporated in SLN nanoparticles was the highest amongst the incorporated compounds? EE and LC were almost the same in any case.

**A:** In accordance with the Reviewer's suggestion, the authors revised the experimental data and we realized that the % inhibition value, at the concentration of 1.03  $\mu$ M (see supporting material), was not considered. This caused an  $IC_{50\pm SD}$  [ $\mu$ M] calculation error regarding the encapsulated Hyt (as can be seen from the graph of the supporting material which has been replaced). The new value is 2.67  $\mu$ M which is not very different from calculated value for other encapsulated PCs.



Click here to access/download  
**Supplementary Material**  
Supplementary Material.docx





**COVER LETTER to reviewers**

**TITLE: Hydroxytyrosol oleate: a promising neuroprotective nanocarrier delivery system of oleuropein and derivatives**

The manuscript submitted has been prepared according to the journal's 'Instructions for Authors',

On submission of the manuscript, the authors agree not to withdraw the manuscript at any stage prior to publication.

In this work hydroxytyrosyl oleate (HtyOle)- and hydroxytyrosyl oleate (HtyOle)-based solid lipid nanoparticles containing OL, 3,4-DHPEA-EA and Hty (SLN-HtyOle, SLN-HtyOle-OL, SLN-HtyOle-3,4-DHPEA-EA and SLN-HtyOle-Hty respectively), were prepared and characterized for size and loading efficiency. In addition, we evaluated *in vitro* the antioxidant activity of these formulations by DPPH assays and by ROS formation using the SH-SY5Y cell line.

The manuscript was resubmitted after making the corrections.

The authors answered point by point to the questions and suggestions posed by the reviewers

AUTHORS: Monica Nardi,<sup>a,b\*</sup> Steve Brocchini,<sup>a</sup> Satyanarayana Somavarapu<sup>a</sup> Antonio Procopio<sup>b</sup>

<sup>a</sup> *Department of Pharmaceutics, UCL School of Pharmacy, 29–39 Brunswick Square, London WC1N 1AX, UK*

<sup>b</sup> *Department of Health Sciences, Università "Magna Græcia" di Catanzaro, Viale Europa – Campus Universitario "S. Venuta" – Loc. Germaneto - 88100 (CZ), ITALY.*



## Conflicts of Interest

The authors declare no conflict of interest.

Moise Nardi

**Author Statement**

The authors declare that they have no known competing financial interests or personal relationships that could have appeared to influence the work reported in this paper.

The authors declare the following financial interests/personal relationships which may be considered as potential competing interests:

## **Hydroxytyrosol oleate: a promising neuroprotective nanocarrier delivery system of oleuropein and derivatives**

Monica Nardi,<sup>a,b\*</sup> Steve Brocchini,<sup>a</sup> Satyanarayana Somavarapu<sup>a</sup> Antonio Procopio<sup>b</sup>

<sup>a</sup> *Department of Pharmaceutics, UCL School of Pharmacy, 29–39 Brunswick Square, London WC1N 1AX, UK*

<sup>b</sup> *Department of Health Sciences, Università “Magna Græcia” di Catanzaro, Viale Europa – Campus Universitario “S. Venuta” – Loc. Germaneto - 88100 (CZ), ITALY.*

### **Highlights**

- We synthesize hydroxytyrosyl oleate (HtyOle)-based solid lipid nanoparticles containing OL, 3,4-DHPEA-EA and Hty
- The nanoparticles were characterized for loading efficiency, size and antioxidant activity.
- We demonstrated that the increased bioavailability of polyphenolic compounds causes an increase in the antioxidant activity of the compounds themselves